

Theoretical study of stability and optical absorption properties of ferroelectric materials ZnXO_3 (X=Ge, Sn and Pb)

Xing-Yuan Chen^{a,c}, Yu-Hua Yang^a, Guo-Xia Lai^a, Jia Chen^a, Wei-Ling Zhu^{a,b}, Tian-Shu Lai^b, Guo-Ping Luo^a, Yu-Jun Zhao^c, Xiang-Fu Xu^{a,*}

^a Department of Physics, School of Science, Guangdong University of Petrochemical Technology, Maoming, Guangdong, 525000, China

^b State-Key Laboratory of Optoelectronic Materials and Technologies, School of Physics and Engineering, Sun Yat Sen University, Guangzhou, Guangdong, 510275, China

^c Department of Physics, South China University of Technology, Guangzhou, 510640, China

ARTICLE INFO

Keywords:

Stability
Optical absorption property
LN-ZnXO₃ (X = Ge, Sn, and Pb)

ABSTRACT

The chemical potential equilibrium phase diagram and optical absorption properties of ZnXO_3 (X = Ge, Sn, and Pb) of LiNbO₃ type (LN- ZnXO_3) have been calculated by density functional theory. We find that LN- ZnXO_3 (X = Ge, Sn, and Pb) do not form a stable chemical potential area with respect to the binary compounds, but could be stabilized under external pressures. The non-equilibrium chemical potential areas in LN- ZnXO_3 (X = Ge, Sn, and Pb) are in a sequence of $\text{Ge} > \text{Sn} > \text{Pb}$. The calculated tendency of transition pressures and binary impurities compound during the synthesis of LN- ZnXO_3 (X = Ge, Sn and Pb) are consistent with the experimental results, which are explained by the structure and electronic structure analysis. The calculated optical absorption property indicates that LN- ZnPbO_3 could be a good ferroelectric photovoltaic material, while LN- ZnXO_3 (X = Ge, Sn) are a good visible light transparent material. The diversity of the feasible transition between VBM and CBM charge with small band gap play important roles in good performance of optical absorption property in LN- ZnPbO_3 . These inclusions could expand the applications of LN- ZnXO_3 (X = Ge, Sn, Pb).

1. Introductions

Ferroelectric materials have attracted intensive attention since they can be widely used in the preparation of tunable capacitors [1], non-volatile memory [2] and solar cells [3,4]. BiFeO₃ (BFO) with R3c space group becomes the popular ferroelectric materials in current research because it harbors both ferroelectric and magnetic ordering properties at room temperature as called multiferroic materials [5,6]. BFO ferroelectric material with a spontaneous polarization field inside the crystal can generate the ferroelectric photovoltaic effect without pn-junction [4]. But most of the ferroelectric materials possess of large band gaps, which cannot absorb the visible light adequately and leading to low photovoltaic efficiency. In fact, researchers try to make great efforts to search the new high-performance ferroelectric materials since the ferroelectric materials are relatively scarce.

With the improved experimental technology, more and more R3c structure ferroelectric materials have been synthesized, such as FeTiO₃ [7], ZnTiO₃ [8], ScFeO₃ [9], ZnSnO₃ [10], ZnGeO₃ [11] and ZnPbO₃ [12], and so on. Benedek and Fennie found that the ferroelectric

materials of the R3c structure FeTiO₃ and ZnSnO₃ were difficult to synthesize due to the competition of their ilmenite phases [13]. The chemical potential of equilibrium phase diagram of XSnO_3 ferroelectric materials (X = Mn, Zn, Fe, Mg) and XTiO_3 (X = Mn, Fe, Co, Ni) had been calculated by first-principles methods to analyze their stability in our earlier work [14,15]. Gou [16] and Nakayama [17] had found that the R3c structure ZnSnO₃ was stable under 7 GPa by calculating the formation enthalpy of R3c structure ZnSnO₃ under different pressures respectively, in agreement with the experimental results. Lee et al. had calculated the Gibbs free energy of ZnSnO₃ under different temperature and pressure conditions [18]. These new R3c structure ferroelectric material are usually synthesized under high pressure condition with some impurity phases precipitated. For example, LN - ZnGeO_3 is prepared under 30 GPa high pressure and annealing condition with appearance of GeO₂ impurities [11]. LN - ZnSnO_3 is prepared with high pressure of 7 GPa and SnO₂ impurities are generated experimentally [10]. Under the high pressure of 4 GPa, the LN- ZnPbO_3 can be detected but with a large number of PbO₂ impurities [12].

In this paper, the formation energy and electronic structure of LN-

* Corresponding author. Tel.: +86 06682923371.

E-mail address: xuxiangfu@gdupt.edu.cn (X.-F. Xu).

<https://doi.org/10.1016/j.physb.2019.411748>

Received 2 November 2018; Received in revised form 23 September 2019; Accepted 3 October 2019

Available online 7 October 2019

0921-4526/© 2019 Elsevier B.V. All rights reserved.

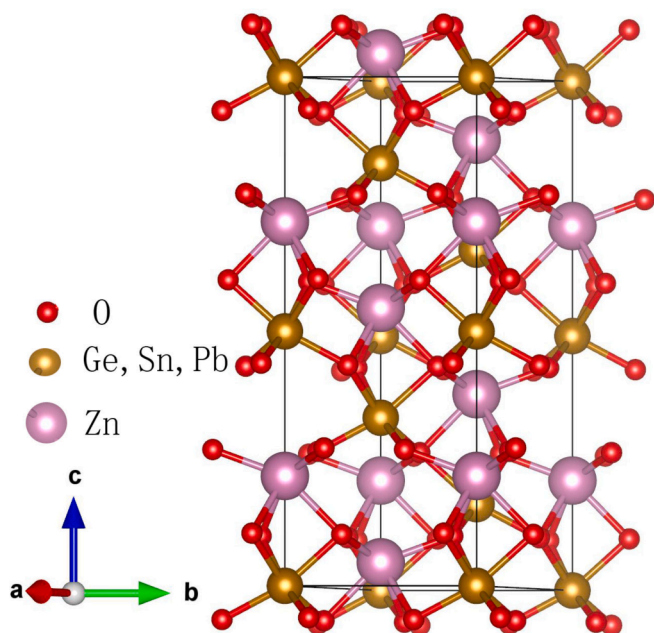


Fig. 1. The structure of LN-ZnXO₃ (X = Ge, Sn and Pb). (For interpretation of the references to colour in this figure legend, the reader is referred to the web version of this article.)

Table 1

The calculated lattice parameters, and corresponding experimental values and relative errors of the ZnXO₃ (X = Ge, Sn, Pb).

	<i>a</i> (Å) ^{cal}	<i>c</i> (Å) ^{cal}	<i>a</i> (Å) ^{exp}	<i>c</i> (Å) ^{exp}	<i>a</i> (relative errors)	<i>c</i> (relative errors)
ZnGeO ₃	4.93	12.72	5.01	13.02	−1.6%	−2.3%
ZnSnO ₃	5.18	13.78	5.26	14.00	−1.5%	−1.6%
ZnPbO ₃	5.33	14.10	5.41	14.33	−1.4%	−1.5%

ZnXO₃ (X = Ge, Sn and Pb) are investigated by first-principles calculations. The high pressure condition and observed impurities in the synthesis of LN-ZnXO₃ (X = Ge, Sn, and Pb) is explained by the chemical potential equilibrium phase diagram. The change of stability of LN-ZnXO₃ (X = Ge, Sn, Pb) are also probed by the transition pressure comparing with reactants and bonding characteristics. The electronic structure calculations show that the absorption of visible light by LN-ZnPbO₃ is more efficient than that of LN-ZnXO₃ (X = Ge, Sn), indicating that LN-ZnPbO₃ is a potential ferroelectric photovoltaic material.

2. Calculation methods

The first-principles calculations were carried out by the VASP package [19] in the framework of density functional calculations, on the basis of the state-of-art functional, Strongly Constrained and Appropriately Normed semilocal (SCAN) functional [20]. The SCAN functional is superior to the traditional LDA and GGA-PBE functional in calculating the total energy and lattice structure for many systems [21]. The cutoff energy for the plane wave basis is set to 550 eV and the Monkhorst-Pack k-points sampling are fixed to 0.02 Å^{−1} for all calculations. The electron configurations of the pseudopotential are chosen as Zn: d10p2, Ge: s2p2, Sn: s2p2, Pb: s2p2 and O: s2p4. The lattice parameters and the atomic coordinates are fully relaxed until Hellman-Feynman forces are less than 0.01 eV/Å. The LN-ZnXO₃ (X = Ge, Sn and Pb) with R3c space group are displayed in Fig. 1. The values of calculated and experimental lattice parameters are listed in Table 1. The relative errors between the calculated and experimental values are about 1.4%–2.3%.

Table 2

The calculated and experimental formation enthalpies of related compounds for LN-ZnXO₃ (X = Ge, Sn, Pb), with the unit in eV.

Compounds	Space group (Number)	Formation enthalpy (cal)	Formation enthalpy (exp)
LN-ZnGeO ₃	161	−8.59	−
LN-ZnSnO ₃	161	−8.99	−
LN-ZnPbO ₃	161	−6.26	−
ZnO	186	−3.33	−3.63
GeO ₂	154	−5.59	−5.70
SnO	129	−2.85	−2.90
SnO ₂	136	−5.82	−5.98
PbO	57	−2.51	−2.26
PbO ₂	136	−2.94	−2.83
Pb ₂ O ₃	14	−5.64	−
Pb ₃ O ₄	135	−8.30	−

3. Results and discussions

3.1. The chemical potential equilibrium phase diagram of LN-ZnXO₃ (X = Ge, Sn and Pb)

In order to obtain the stable LN-ZnXO₃ (X = Ge, Sn and Pb) crystals under thermodynamic equilibrium conditions, the total chemical potential of different types of atoms should be equal to the formation energy of the host compound.

$$\Delta\mu_{Zn} + \Delta\mu_X + 3\Delta\mu_O = \Delta E_f(\text{ZnXO}_3) \quad (1)$$

ΔE_f and $\Delta\mu$ represent the formation energy and chemical potential respectively. The chemical potential of the atom should satisfy the following inequalities to avoid the emergence of the binary competition as impurity.

$$\Delta\mu_{Zn} + \Delta\mu_O \leq \Delta E_f(\text{ZnO})$$

$$\Delta\mu_{X_i} + \Delta\mu_{O_j} \leq \Delta E_f(\text{X}_i\text{O}_j) \quad (2)$$

$\Delta E_f(\text{ZnO})$ and $\Delta E_f(\text{X}_i\text{O}_j)$ are the formation energies of the competing binary phases in the LN-ZnXO₃ (X = Ge, Sn and Pb), including ZnO, TiO₂, Ti₂O₃, GeO₂, SnO, SnO₂, PbO, PbO₂, Pb₂O₃, Pb₃O₄. The calculated formation energy of various compounds are shown in Table 2, and the calculated values and experimental values for most of the binary competitive phases are in line with each other, implying the reliability of our calculation. As shown in Fig. 2, the chemical potential equilibrium phase diagram of LN-ZnXO₃ (X = Ge, Sn and Pb) can be acquired by Equations (1) and (2) and the data of Table 2. The vertical and lateral axes in Fig. 2(a)–(c) are the chemical potential of X (Ge, Sn and Pb) and Zn atoms respectively. The large triangle BD side is the chemical potential of O atom with zero value. The right above region of the line is the allowed region of existence of LN-ZnXO₃ structures. Fig. 2 (d)–(f) shows that LN-ZnXO₃ (X = Ge, Sn, and Pb) do not form a stable chemical potential area since Equations (1) and (2) can not satisfy concurrently. Similar case with LN-XSnO₃ (X = Mn, Fe, Mg) and LN-XTiO₃ (X = Mn, Fe, Co, Ni), the lack of stable chemical potential area implies that LN-ZnXO₃ (X = Ge, Sn, and Pb) could not be synthesized by general thermodynamic equilibrium conditions and may require non-equilibrium methods like high pressure. As further seen from Fig. 2, the unstable chemical potential range of LN-ZnXO₃ (X = Ge, Sn, and Pb) is mainly depending on AB (ZnO) and CD (GeO₂, SnO₂, and PbO₂) in LN-ZnXO₃ (X = Ge, Sn, and Pb). The non-equilibrium area enclosed by ABCD (Fig. 2) is Ge > Sn > Pb correspondingly, which means that Ge deviates from the equilibrium state more severely and requiring a higher pressure to maintain a stable LN-ZnGeO₃. The pressure required by stable LN-ZnXO₃ (X = Sn, Pb) decreases gradually since the non-equilibrium area ABCD become smaller. In fact, the preparation of LN-ZnXO₃ (X = Ge, Sn, and Pb) were performed using ZnO + (GeO₂, SnO₂, and PbO₂) reactions assisted by the high pressure experimentally. LN-

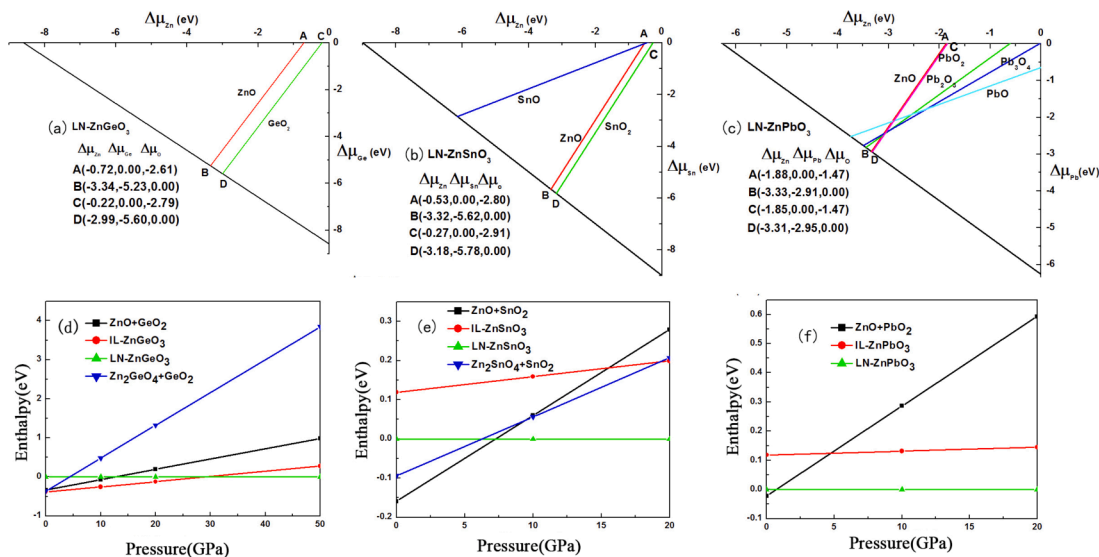


Fig. 2. The calculated equilibrium chemical potential phase diagram and the formation enthalpy under various pressure with their major competing phases of LN-ZnXO₃ (X = Ge, Sn, and Pb). (For interpretation of the references to colour in this figure legend, the reader is referred to the web version of this article.)

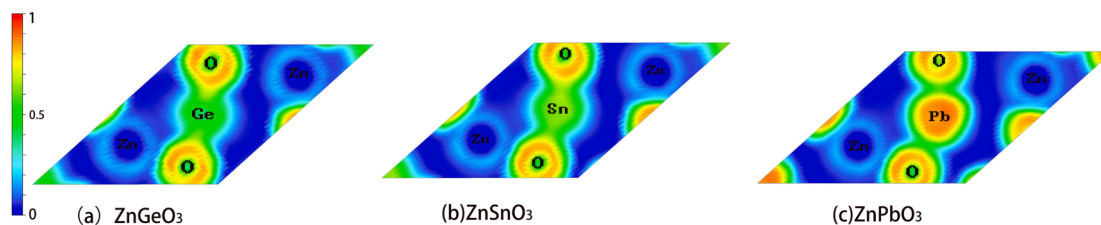


Fig. 3. The ELF charge of LN-ZnXO₃ (X = Ge, Sn, and Pb) at (111) plane. (For interpretation of the references to colour in this figure legend, the reader is referred to the web version of this article.)

ZnGeO₃ is synthesized under 30 GPa high pressure with annealing conditions, while LN-ZnSnO₃ is stable at 7 GPa and LN-ZnPbO₃ is already available at 4 GPa, indicating that the analysis of chemical potential phase diagram are consistent with the trend of experimental pressure results. The GeO₂, SnO₂, and PbO₂ impurities are easily precipitated during the preparation process of LN-ZnXO₃ (X = Ge, Sn, and Pb), while ZnO impurities are less. From the values of Zn, Ge, Sn, Pb, and O chemical potentials in Fig. 2, it can be seen that the chemical potential range of Ge, Sn, or Pb is larger than that of Zn. The GeO₂, SnO₂ and PbO₂ compounds could be produced regardless of rich or poor condition and become the main impurities during the synthesis of LN-ZnXO₃ (X = Ge, Sn and Pb), which are consistent with the experimental results. At the same time, the formation enthalpy of LN-ZnXO₃ (X = Ge, Sn, and Pb) and some of their major competing phases including some binary competitor, ternary competitor, and ilmenite structure ZnXO₃ are calculated with different pressure, as shown in Fig. 2. The enthalpy of LN-ZnXO₃ and competitive phase compounds under different pressures are acquired by formula $H = E_0 + PV$. H and P represent the enthalpy and the external pressures. E_0 and V are the energy and volume under zero pressure given by first-principles. Through the simple formula $H = E_0 + PV$, the estimated transition pressures are basically consistent with experimental variation tendency and early literature calculations. The calculated results show that the transition pressures appearing in the LN-ZnXO₃ (X = Ge, Sn, and Pb) phases are 29.1, 7.2, and 1.1 GPa respectively, while the transition pressures of appearance of LN-ZnXO₃ (X = Ge, Sn, and Pb) are 30, 7 and 4 GPa in the experiments [10–12]. Our calculated transition pressures results of LN-ZnXO₃ (X = Ge, Sn) are basically consistent with experimental tendency [10–12] and early calculations in literature [16–18]. The calculated transition pressures results of LN-ZnPbO₃ has certain deviations from the experimental

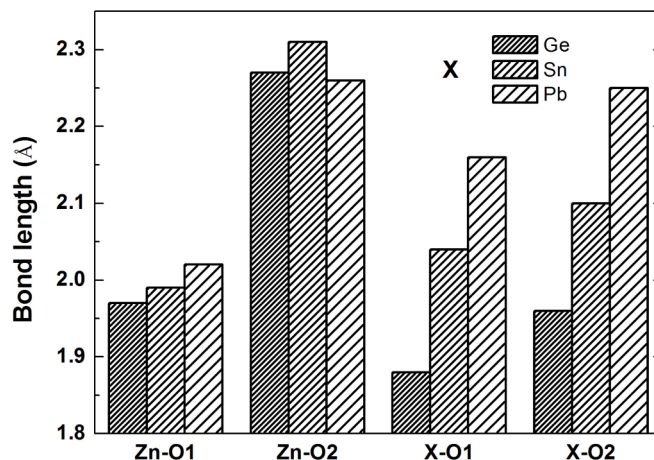


Fig. 4. The distribution of bond length of LN-ZnXO₃ (X = Ge, Sn and Pb).

values, which could be due to the existence of some complicated ternary competition phases in the actual experiment process [12]. In general, the calculated chemical potential phase diagram and the formation enthalpy with various pressures indicate that the LN-ZnXO₃ (X = Ge, Sn, and Pb) could be synthesized under high pressure condition. The calculated transition pressures of the LN-ZnXO₃ (X = Ge, Sn, and Pb) during the synthesis process are close to the experimental values and tendency. The stability of LN-ZnXO₃ (X = Ge, Sn) are also related with their bond type and bond length. The electron localization function (ELF) charge (Fig. 3) indicates that the charge of Zn are localized to form

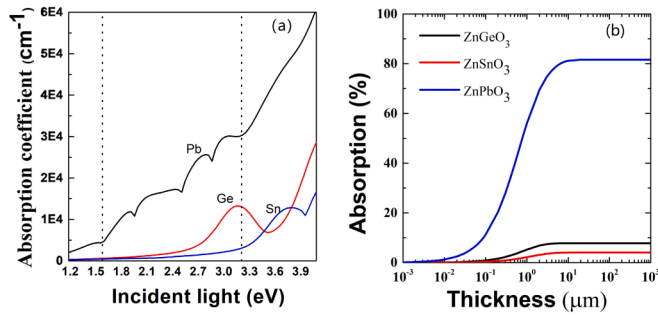


Fig. 5. The absorption coefficient (a) and the total fractional absorption (b) of LN-ZnXO₃ (X = Ge, Sn and Pb). (For interpretation of the references to colour in this figure legend, the reader is referred to the web version of this article.)

Table 3

The calculated band gap values (in eV) of LN-ZnXO₃ (X = Ge, Sn, Pb) by different functionals.

Compounds	MBJ (present)	GGA	HSE	GW
ZnGeO ₃	2.91	1.30 ^{ref [25]}	—	—
ZnSnO ₃	3.16	2.42 ^{ref [26]}	3.02 ^{ref [24]}	3.72 ^{ref [24]}
ZnPbO ₃	1.09	—	1.13 ^{ref [24]}	1.45 ^{ref [24]}

ionic bond and the charge of X (X = Ge, Sn, and Pb) and O are partly non-localized along with sharing some charge to form ionic bond and segmental covalent bond. Covalent bonds are more resistant to external pressure than ionic bonds commonly. The statistical distribution of bond length of LN-ZnXO₃ (X = Ge, Sn) are shown in Fig. 4. Among the LN-ZnXO₃ (X = Ge, Sn) system, the bond lengths of Ge-O and Zn-O are the shortest to present strong interaction to resist the external pressure, while the bond length of Pb-O are largest along with weak interaction to resist the external pressure relatively.

3.2. Optical absorption property

As shown in Fig. 5(a), the absorption coefficient of the LN-ZnXO₃ (X = Ge, Sn and Pb) have been calculated near the visible range. The absorption coefficient $\alpha(\omega)$ is given as follows.

$$\alpha(\omega) = \sqrt{2}\omega \left[\sqrt{\epsilon_1(\omega)^2 + \epsilon_2(\omega)^2} - \epsilon_1(\omega) \right]^{\frac{1}{2}} \quad (3)$$

$\epsilon_1(\omega)$ and $\epsilon_2(\omega)$ are the real and imaginary parts of the dielectric function, respectively. With the absorption coefficient $\alpha(E)$ and film thickness d , the total fractional absorption A (Fig. 5(b)) of incident solar radiation can be approximated as

$$A(\%) = \left(1 - \frac{\int_0^{E_g} S_E dE}{\int_0^\infty S_E dE} - \frac{\int_{E_g}^\infty e^{-\alpha(E)d} S_E dE}{\int_0^\infty S_E dE} \right) \times 100 \quad (4)$$

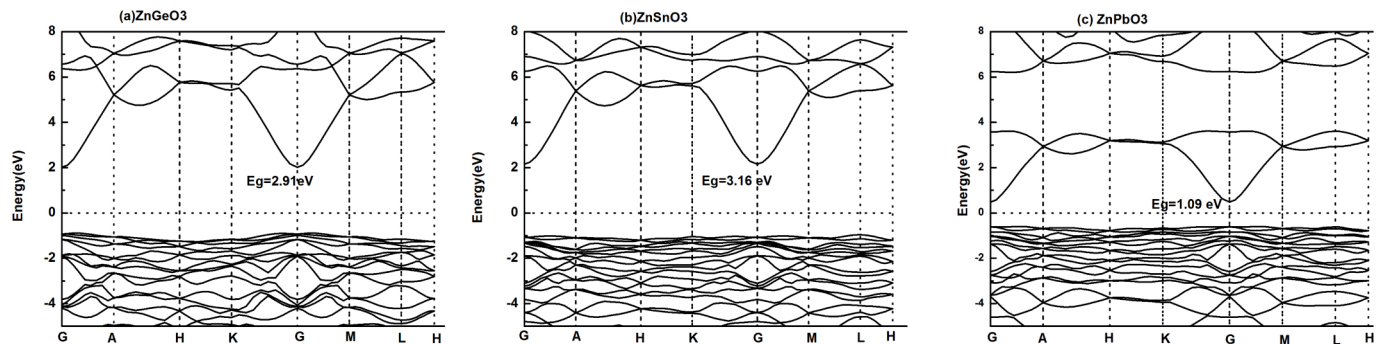


Fig. 6. The energy band structure of LN-ZnXO₃ (X = Ge, Sn and Pb).

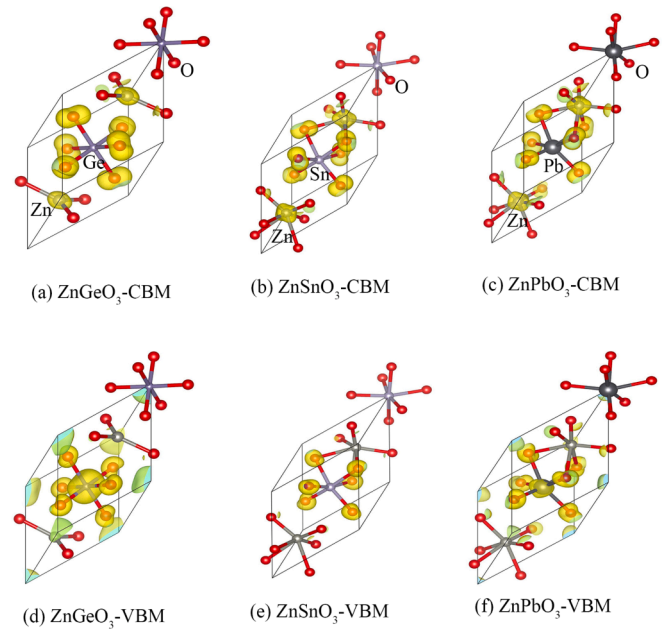


Fig. 7. The VBM and CBM charge distribution of LN-ZnXO₃ (X = Ge, Sn and Pb). (For interpretation of the references to colour in this figure legend, the reader is referred to the web version of this article.)

Where S_E is the incident solar spectral irradiance as a function of the photon energy E , and E_g is the band gap. At $9 \mu\text{m}$ thickness, the light absorption ratio of ZnGeO₃ begins to saturate and reaches to 7.76%. The light absorption ratio of ZnSnO₃ is relatively small, and the saturated light absorption ratio is 4.06% with $20 \mu\text{m}$ thickness. The saturated light absorption ratio of ZnPbO₃ becomes the highest at $10 \mu\text{m}$ thickness and reaches to 81.19%. The calculated results show that absorption coefficient of LN-ZnPbO₃ is higher than that of LN-ZnXO₃ (X = Ge and Sn) in the visible light range, which is conducive to absorb visible light. The band structures of LN-ZnXO₃ (X = Ge, Sn and Pb) have been calculated by the Modified Becke-Johnson (MBJ) functional, which could usually obtain accurate band gap, consistent with the results of hybrid functional or GW functional [22,23]. As shown in Table 3 and Fig. 6, the band gap values of LN-ZnXO₃ (X = Ge, Sn and Pb) are 2.91, 3.16 and 1.09 eV, respectively, which are consistent with the early results of HSE06 functional calculation [24], while the traditional GGA calculations underestimate the band gap [25,26]. The small band gap of LN-ZnPbO₃ takes advantage to absorb more visible light, which leads to potential ferroelectric photovoltaic properties and consistent with the early literature report [24]. However, the band gap of LN-ZnXO₃ (X = Ge and Sn) are relatively large along with small absorption coefficient and total fractional absorption to reduce absorption of visible light. LN-ZnXO₃ (X = Ge, Sn) with large band gap and some carrier

doping could be a good transparent electrode material, which is agreement with the early report on the ZnSnO₃ as a transparent electrode material [27]. As shown in Fig. 7, the valence band maximum (VBM) charge of LN-ZnXO₃ (X = Ge, Sn and Pb) are mainly composed by Zn-3d and O-2p levels. The conduction band minimum (CBM) of LN-ZnSnO₃ is mainly composed by O-2p level. The optical transition between Zn-3d and O-2p orbits could be occurred in the LN-ZnSnO₃ material. The CBM charge of LN-ZnGeO₃ is mainly composed by Ge-4p level and O-2p level. The optical transition of Zn-3d to O-2p, Zn-3d to Ge-4p, and O-2p to Ge-4p could appear in the LN-ZnGeO₃ material. In LN-ZnPbO₃, CBM charge is mainly occupied by the Pb-6p and O-2p. The CBM charge of LN-ZnPbO₃ is mainly occupied by Pb-6p level and O-2p level. The optical transition of Zn-3d to O-2p, Zn-3d to Pb-6p, and O-2p to Pb-6p could appear in the LN-ZnPbO₃ material. Therefore, the small band gap of LN-ZnPbO₃ and the diversity of the feasible transition between VBM and CBM charge could enhance the absorption of visible light.

4. Conclusions

In summary, the chemical potential equilibrium phase diagram and optical absorption property of LN-ZnXO₃ (X = Ge, Sn, and Pb) have been studied by the first-principles calculations. The calculated chemical potential equilibrium phase diagram indicates that LN-ZnXO₃ (X = Ge, Sn, and Pb) have no stable chemical potential area with respect to the competition of binary compounds. The relationships of non-equilibrium chemical potential area in LN-ZnXO₃ (X = Ge, Sn, and Pb) are Ge > Sn > Pb, which means that Ge deviates from the equilibrium state more severely and requiring a higher pressure to maintain LN-ZnGeO₃ stable. The pressure required by LN-ZnXO₃ (X = Sn, Pb) decreases gradually since the non-equilibrium area become smaller. The calculated transition pressures comparing with the reactants in the LN-ZnXO₃ (X = Ge, Sn, and Pb) phases are basically consistent with experimental variation tendency. The Zn-O bonds mainly form ionic bond, while Ge-O, Sn-O, and Pb-O could form ionic bond and segmental covalent bond in LN-ZnXO₃ (X = Ge, Sn, and Pb) by the ELF analyze. The bond length of Ge-O and Zn-O in LN-ZnGeO₃ are shortest to present strong interaction to resist the external pressure, while the bond length of Pb-O are largest along with weak interaction to resist the external pressure relatively. The calculated band gap values of LN-ZnXO₃ (X = Ge, Sn and Pb) are 2.91, 3.16 and 1.09 eV respectively. In LN-ZnPbO₃, CBM are mainly contributed by the Pb-6p and O-2p levels, while VBM charges are mainly attributed to Zn-3d and O-2p levels. The optical transition of Zn-3d to O-2p, Zn-3d to Pb-4p, O-2p to Pb-6p could appear in LN-ZnPbO₃. The diversity of the feasible transition between VBM and CBM charge with small band gap in LN-ZnPbO₃ could enhance the absorption of visible light.

Declaration of competing interest

There are no conflicts of interest.

Acknowledgements

This work was supported by the NSFC (Grant No. 11547201, 61475195), Natural Science Foundation of Guangdong Province, China

(Grant No. 2017A030307008).

References

- [1] A. Jamil, T.S. Kalkur, N. Cramer, Tunable ferroelectric capacitor-based voltage-controlled oscillator, *IEEE Trans. Son. Ultrason.* 54 (2) (2007) 222.
- [2] V. Garcia, M. Bibes, Electronics: inside story of ferroelectric memories, *Nature* 483 (7389) (2012) 279.
- [3] T. Choi, S. Lee, Y.J. Choi, et al., Switchable ferroelectric diode and photovoltaic effect in BiFeO₃, *Science* 324 (5923) (2009) 65.
- [4] S.Y. Yang, J. Seidel, S.J. Byrnes, et al., Above-band gap voltages from ferroelectric photovoltaic devices, *Nat. Nanotechnol.* 5 (2) (2010) 143.
- [5] J. Wang, J.B. Neaton, H. Zheng, et al., Epitaxial BiFeO₃ multiferroic thin film heterostructures, *Science* 307 (24) (2003) 1719.
- [6] W. Eerenstein, N.D. Mathur, J.F. Scott, Multiferroic and magnetoelectric materials, *Nature* 442 (7104) (2006) 759.
- [7] T. Varga, A. Kumar, E. Vlahos, et al., Coexistence of weak ferromagnetism and ferroelectricity in the high pressure LiNbO₃-type phase of FeTiO₃, *Phys. Rev. Lett.* 103 (4) (2009), 047601.
- [8] Y. Inaguma, A. Aimi, Y. Shirako, et al., High-pressure synthesis, crystal structure, and phase stability relations of a LiNbO₃-type polar titanate ZnTiO₃ and its reinforced polarity by the second-order Jahn-Teller effect, *J. Am. Chem. Soc.* 136 (7) (2014) 2748.
- [9] T. Kawamoto, K. Fujita, I. Yamada, et al., Room-temperature polar ferromagnet SrFeO₃ transformed from a high-pressure orthorhombic perovskite phase, *J. Am. Chem. Soc.* 136 (43) (2014) 15291.
- [10] Y. Inaguma, M. Yoshida, T. Katsumata, A polar oxide ZnSnO₃ with a LiNbO₃-type structure, *J. Am. Chem. Soc.* 130 (21) (2008) 6704.
- [11] H. Yusa, M. Akaogi, N. Sata, et al., High-pressure transformations of ilmenite to perovskite, and lithium niobate to perovskite in zinc germanate, *Phys. Chem. Miner.* 33 (33) (2006) 217.
- [12] R. Yu, H. Hojo, T. Mizoguchi, et al., A new LiNbO₃-type polar oxide with closed-shell cations: ZnPbO₃, *J. Appl. Phys.* 15 (9) (2015) 710.
- [13] N.A. Benedek, C.J. Fennie, Why are there so few perovskite ferroelectrics? *J. Phys. Chem. C* 117 (26) (2013) 13339.
- [14] Weilong Zhu, Xingyuan Chen, Yujun Zhao, et al., Theoretical study of stability and electronic structure of the new type of ferroelectric materials XSnO₃ (X = Mn, Zn, Fe, Mg), *Int. J. Mod. Phys. B* 28 (31) (2014), 1450224.
- [15] Xingyuan Chen, et al., First-principles study on the stability and magnetoelectric properties of multiferroic materials XTiO₃ (X = Mn, Fe, Co, Ni), *Int. J. Mod. Phys. B* 32 (9) (2018), 1850105.
- [16] H. Gou, J. Zhang, Z. Li, et al., Energetic stability, structural transition, and thermodynamic properties of ZnSnO₃, *Appl. Phys. Lett.* 98 (9) (2011), 091914.
- [17] M. Nakayama, M. Nogami, M. Yoshida, et al., First-principles studies on Novel polar oxide ZnSnO₃; pressure-induced phase transition and electric properties, *Adv. Mater.* 22 (23) (2010) 2579.
- [18] J. Lee, S.C. Lee, C. Hwang, et al., Thermodynamic stability of various phases of zinc tin oxides from ab initio calculations, *J. Mater. Chem. C* 1 (39) (2013) 6364.
- [19] G. Kresse, J. Furthmüller, Efficiency of ab-initio total energy calculations for metals and semiconductors using a plane-wave basis set, *Comput. Mater. Sci.* 6 (1) (1996) 15.
- [20] J. Sun, A. Ruzsinszky, J.P. Perdew, Strongly constrained and appropriately Normed semilocal density functional, *Phys. Rev. Lett.* 115 (3) (2015), 036402.
- [21] J. Sun, R.C. Remsing, Y. Zhang, et al., Accurate first-principles structures and energies of diversely bonded systems from an efficient density functional, *Nat. Chem.* 8 (9) (2016) 831.
- [22] A.D. Becke, E.R. Johnson, A simple effective potential for exchange, *J. Chem. Phys.* 124 (22) (2006) 317.
- [23] F. Tran, P. Blaha, Accurate band gaps of semiconductors and insulators with a semilocal exchange-correlation potential, *Phys. Rev. Lett.* 102 (22) (2009) 226401.
- [24] J. He, C. Franchini, J.M. Rondinelli, Lithium niobate-type oxides as visible light photovoltaic materials, *J. Chem. Mater.* 28 (1) (2016) 25.
- [25] J. Zhang, B. Xu, Z. Qin, et al., Ferroelectric and nonlinear optical properties of the LiNbO₃-type ZnGeO₃, from first-principles study, *J. Alloy. Comp.* 514 (7) (2012) 113.
- [26] H. Gou, F. Gao, J. Zhang, Structural identification, electronic and optical properties of ZnSnO₃: first principle calculations, *Comput. Mater. Sci.* 49 (3) (2010) 552.
- [27] K.P. Ong, X. Fan, A. Subedi, et al., Transparent conducting properties of SrSnO₃ and ZnSnO₃, *J. APL. Mater* 3 (6) (2015) 15.